VIBANASS (VISION BASED NAVIGATION SENSOR SYSTEM) SYSTEM TEST RESULTS

G. Hausmann[(1)], Q. Mühlbauer[(1)], P. Rank[(1)], C. Kaiser[(1)]

[(1)] Kayser-Threde GmbH, Wolfratshauser Str. 48, 81379 Munich, Germany,
Email: gerrit.hausmann@kayser-threde.com

ABSTRACT

Future Active Debris Removal missions will require vision sensors both to support guidance, navigation and control and to examine the targeted debris object prior to capture. With this scenario in mind, Kayser-Threde has developed the VIsion BAsed NAvigation Sensor System (VIBANASS). A demonstrator model representative of the flight hardware was built for execution of a space qualification program and subjected to an extensive test campaign at the European Proximity Operations Simulator (EPOS). It was shown that VIBANASS is able to perform its tasks reliably in vision-based Rendezvous and Docking maneuvers under a wide variety of illumination conditions. These tests included image processing algorithms for target distance evaluation and a closed-loop rendezvous experiment.

1 INTRODUCTION

Several orbital regions around Earth are so highly populated with space debris that Active Debris Removal (ADR) missions will be necessary to avoid cascading collision effects which may eventually leave key orbits unusable [1]. For such ADR missions, a vision system is important for rendezvous with debris objects and essential for their detailed inspection prior to capture. Furthermore, distance and attitude information of the target are required for the capture algorithms.

For this scenario, Kayser-Threde has developed the VIsion BAsed NAvigation Sensor System (VIBANASS) [2, 3]. It consists of two Camera Systems (CS), a Target Illumination System (TIS) and a Ground Operation System (GOS). Each Camera System includes three cameras, optimized for far-range (3 km to 75 m), mid-range (500 m to 4.5 m) and close-range (5.5 m to 0.7 m) operations. In close-range, two cameras are operated in a stereo configuration with a stereo base of 0.5 m. The laser-based Target Illumination System is a highly modular assembly, supporting a wide range of different optical power configurations called for by the different application requirements.

A first test campaign with a breadboard model of VIBANASS under representative illumination conditions was conducted in December 2011 [4] at the EPOS facility [5], proving the general concept.

Following this, a demonstrator model representative of the flight hardware was built and subjected to a further and more elaborate test campaign in early 2013. This campaign included functional and performance tests, the results of which are presented in this paper. Distance determination data of a dedicated image processing [6] ground software was used for verification and evaluation of the performance of VIBANASS. The software applies target-specific distance estimation algorithms and uses the VIBANASS camera images as input. Besides being used for evaluation of the VIBANASS performance, the algorithms were also used as input for a closed-loop Rendezvous-and-Docking control algorithm in an additional test.

2 VISION BASED NAVIGATION SENSOR SYSTEM

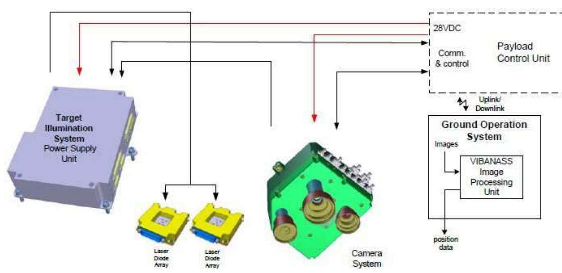

Figure 1. VIBANASS Subsystems and Interfaces

Fig. 1 shows the operational scenario of VIBANASS with one Camera System (CS), the Target Illumination System (TIS) and the Ground Operation System (GOS) in flight configuration. The VIBANASS demonstrator equipment was designed for an operational temperature range of -40°C to +50°C and a non-operational range of -40°C to +85°C. The design is radiation tolerant (TID: 100 KRad(Si), LET: 80 MeV cm²/mg). The subsystems of VIBANASS will be presented in detail in the next sections.

2.1 Camera System

The VIBANASS Camera System comprises all necessary hardware for the operation of three CMOS Sensors, communication interfaces, hardware controller and a power-supply module. Each

Proc. '6th European Conference on Space Debris'
Darmstadt, Germany, 22–25 April 2013 (ESA SP-723, August 2013)

camera system supports a resolution of up to 1024x1024 pixels. A common housing accommodates all electronics and optics for the three different camera heads. Core functions and features of the Camera System are:

- Redundant SpaceWire Interface Encoder/Decoder
- Individual control of each camera head
- Synchronization for stereo camera
- Image acquisition rate: max 10 Hz
- Lossy and lossless JPEG compression
- Configurable image size
- Synchronization with Target Illumination System
- Simultaneous operation of 2 camera heads (stereo image acquisition)
- Optional Image Processing Module (internal Add-on Module for image pre-processing functions)
- Power consumption: 28 V / 5 W
- 4.8 kg for GEO application and 3.7 kg for LEO
- Size of CS: 251 mm x 237 mm x 215 mm

2.2 Target Illumination System

The laser-based VIBANASS Target Illumination System (TIS) is designed to illuminate the whole field of view of the VIBANASS Close-Range Camera from a distance of 5 m with an optical power of at least 10% of natural sunlight. Therefore the Close-Range Camera's spectral bandwidth corresponds to the wavelength (808 nm) of the laser-based illumination system within the specified environment. Due to its modularity, other applications can also easily be served.

A TIS Module consists of a Power Supply Unit (TIS-PSU) and two Laser Diode Arrays (TIS-LDA) with 8 W optical power for each. Several TIS-Modules can be operated in parallel. Using dedicated hardware lines the TIS power output can be synchronized with the VIBANASS Camera System for energy saving. Furthermore, the output power can be remotely controlled by digital control. Isolated safety inhibit signal lines support ground operation safety.

The TIS-LDA was successfully tested with a TID of 235 KRad(Si) and with 3.1E11 protons/cm^2 @ 30 MeV.

Its physical parameters are:

- Size of TIS-PSU: 169 mm x 106 mm x 40 mm
- Size of TIS-LDA: 70 mm x 76 mm x 20 mm
- 2.05 kg (incl. 2 LDA's) for GEO, 1.65 kg for LEO
- Power consumption: 28 V / 15 W @ 16 W optical power and 10% duty cycle

2.3 Ground Operation System

In addition to the hardware, the Ground Operation System (GOS) comprises software to command the VIBANASS equipment, to receive and decompress images and finally to estimate the position of the target in real-time. For this purpose, it performs frame-to- frame tracking by using a geometric model, and it is capable of automatic re-initialization in case of loss.

Object detection consists of a global search, in order to localize the given shape (rectangle, circle) in full 3D space, within the whole range of distances and horizontal, vertical positions [3]. This procedure is computationally intensive and less accurate than tracking, and can also provide false positives (the object is found in the wrong location) or missing detections.

The tracking procedure, instead, consists of a local search, that requires a predicted pose. In absence of a dynamic model, the prediction is simply given by the estimate from the previous frame. The edge-based tracking procedure is based on a local search for nearest-neighbor edges, along the normals to the contour. Least-squares errors are minimized using a robust estimator and the procedure is iterated until convergence.

3 TEST SETUP

The general test setup is shown in Fig. 2. It consists of the target mock-up mounted on the left robot and the VIBANASS equipment mounted on the right robot. This robot is mounted on a rail for movement in line-of-sight direction. The sun simulator is shown on the right side of the image and is a 12 kW spotlight with a sun like spectrum and comparable optical power.

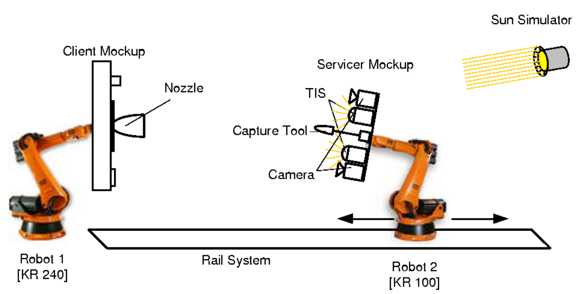

Figure 2. General Test Setup

Fig. 3 shows the setup with the two VIBANASS cameras and parts of the Ground Operation System:

- Two Camera Systems, mounted on the top left and on the top right
- Capture Tool, a servicing tool on the chaser satellite
- TIS-Power Supply Unit, mounted on

the bottom right
- Two TIS-LDA's, mounted between the Camera Systems and between the TIS-PSU and the GOS
- Ground Operation System, mounted on the lower left

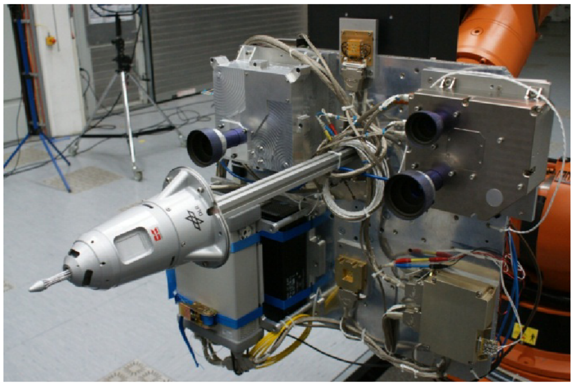

Figure 3. VIBANASS mounted on the chaser

Both Close-Range Cameras are used as a stereo camera system with a stereo base of 0.5 m. The Ground Operation System mounted on the robot is made up of a computer and the digital interface, emulating an on-board computer on a satellite. Results of the image processing algorithm are computed in a reference frame located in the focal point of the left Close-Range Camera for the stereo case and in the focal point of the left Mid-Range camera for the mono case. The line of sight marks the z-axis and the camera horizon marks the x-axis.

Figure 4. Target Mock-Up

Fig. 4 shows the mock-up of the target, which is illuminated by the sun simulator. The target frame is located in the center of the nozzle's exit-plane.

As described in Tab. 1, different trajectories have been used for the tests, starting at a distance of 25 m and ending at the parking position at a distance of 0.5 m. The distance is measured in z-direction between the camera frame and the target frame.

Table 1. Description of the trajectories

ID	Description	Duration
N1	Linear movement from 25 m to 0.5 m Station keeping for 120 s at a distance of 5 m (in x-direction)	~15 min
N2	N1 + sinusoidal rotation around the y_S-axis	~13.5 min
N3	N2 + linear rotation around the x_S-axis from	~13.5 min
S1	Fixed position at 5 m. Sinusoidal rotation around the y_S-axis	~5 min
S2	S1 + sinusoidal movement in y_S direction	~5 min

These trajectories cover nominal as well as non-nominal cases and are used under different illumination conditions. The linear movement in N1 covers the nominal case, while the movements with a relatively large displacement in N2 and the sinusoidal oscillation around the y-axis in N3 mark the non-nominal cases, imposing a challenge to the robustness of the image processing. All trajectories were accelerated by a factor of 5 relative to real mission conditions which increased the number of illumination conditions that could be tested in a reasonable amount of time. The image processing algorithm was expected to have a larger error in the non-nominal cases, while the image quality remains constant. The different trajectories were simulated with four different positions of the sun simulator and with five different illumination settings.

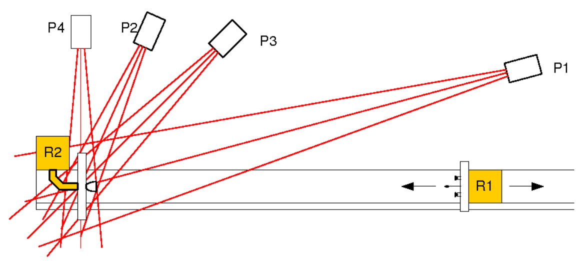

Figure 5. Different positions of the sun simulator

Fig. 5 shows the four different positions of the sun simulator. The positions differ in the angle between the camera line of sight and the sun simulator. In addition to, a test case without the sun was defined.

Before performing the actual tests the illumination conditions were calibrated. For this, the sensor head of an optical power meter was mounted on the target mock-up, the sun simulator was placed at the given positions, and the brightness was adjusted until the desired ratio between the irradiance achieved by the sun simulator and the irradiance achieved by the Target Illumination System was measured. In a flight-like setting, the Target Illumination System is able to illuminate with an optical power of 10% of the sunlight at a distance of 5 m. This value was estimated by a radiometric analysis and verified during the first breadboard test campaign at EPOS. Tab. 2 shows a list of the optical power of the Target Illumination System and the sun simulator.

Table 2. Achieved ratio between sun simulator and Target Illumination System

Desired Ratio	**20%**	**10%**	**5%**
Sun intensity [W/m²]	8.1	11.9	15.9
TIS intensity [W/m²]	1.64	1.13	0.73
Achieved ratio	20.2%	9.5%	4.6

A total of 53 test cases were selected for the test campaign, varying the trajectory, the position of the sun and the illumination setting. Thus, a wide variety of environmental conditions was achieved. Fig. 6 shows the approach of trajectory N1 at a distance of 15 m and 0.5 m as seen by a surveillance camera. The surveillance camera is sensitive to infrared light, so the operator is able to see the laser of the TIS.

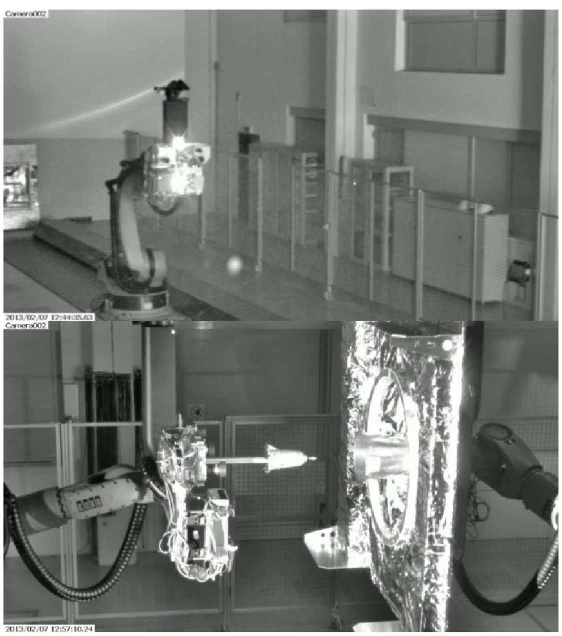

Figure 6. Approach seen by a surveillance camera

4 TEST RESULTS

This section describes the major results from the EPOS tests, starting with example images recorded by the Camera System under different illumination conditions and configurations. Image quality and performance of the image processing algorithm are evaluated, followed by a brief summary of the closed-loop tests.

4.1 Example Images

Fig. 7 compares images recorded by the Close- and Mid-Range Camera under good (sun mostly behind the chaser) and bad (sun light from the side) illumination conditions. The images have been recorded at distances of 5 m and 2 m by the Close-Range Camera and the Mid- Range Camera, respectively.

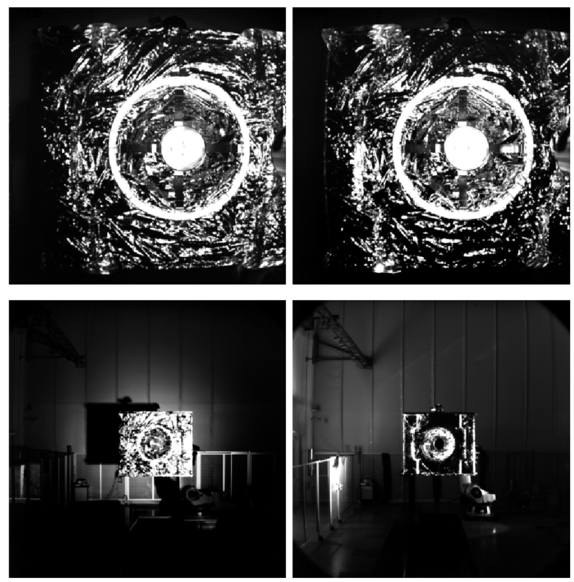

Figure 7. Good (left) and bad (right) illumination conditions seen by the CAM-CR (top row) and the CAM-MR (bottom row)

Fig. 8 shows the impact of the image compression for the Close- and the Mid-Range Camera. The left column shows images with a high compression and the right with a low compression setting. As expected, high compression leads to a poor image quality. The difference between lossless and low compression rates cannot be recognized by the human eye. All images have been recorded at a distance of 5 m for the Close- Range Camera and 20 m for the Mid-Range Camera.

Low compression is optimized for sending a stereo image pair at full resolution with a communication bandwidth of 4 Mbit, which is a typical for a LEO application. High image compression is optimized for a communication channel with a bandwidth of 0.4 Mbit, a typical value for a chaser's S-Band link in GEO.

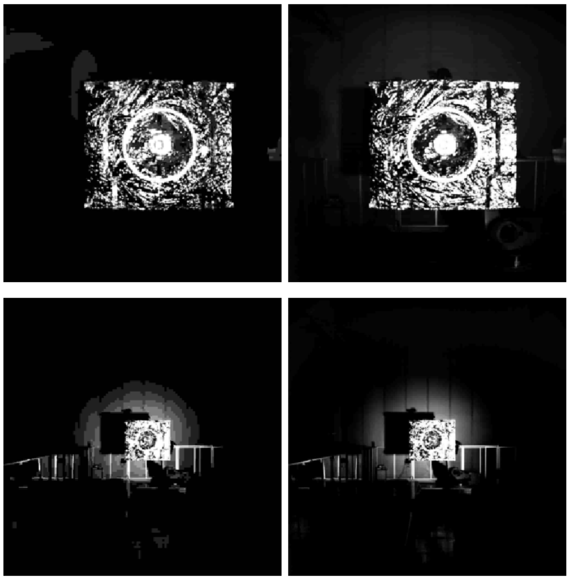

Figure 8. High (left) and low (right) image compression

Fig. 9 illustrates the impact of the TIS by showing images recorded under different brightness settings (from upper left to lower right): no active TIS, illumination ratio of 5%, illumination ratio of 20% and no sun simulator. Note that the exposure time has been adjusted to increase the overall image quality, so the brightness seems comparable. All images have been recorded at a distance of 5 m.

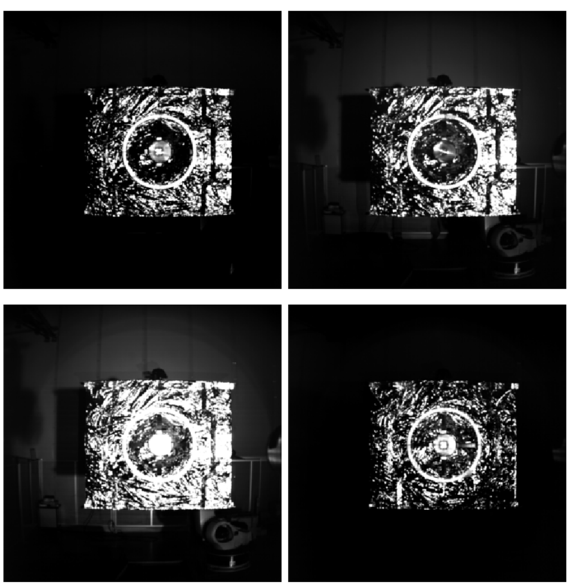

Figure 9. Impact of the TIS

Not only the quality of the images and the positions error of the image processing algorithm is important, but also the delay induced by the whole system. The results show, that the delay is depending on the compression rate and ranges between 350 ms for an lossless image and 20 ms for high compression.

4.2 Evaluation of Image Quality

A total of 53 test cases has been conducted during the EPOS tests. The following image quality factors have been analyzed for each image recorded during the tests:

- Signal to Noise Ratio
- Sharpness/blur
- Image contrast

The image quality has been evaluated for each test case, which mainly differ in the illumination conditions. To permit a reliable statement, the test cases have been separated into three categories:

- All test cases are included in the category mean illumination conditions.
- Challenging conditions are combined in the category bad illumination conditions. Those include test sequences with no sun simulation, large angles between the line of sight and the sun simulator or flights without the TIS.
- Favorable conditions are those with the sun coming from the back and with nominal TIS. They are combined in the category good illumination conditions.

The signal to noise ratio of the cameras was computed using the mean absolute deviation algorithm. For this, the image is separated into small windows, in which the noise is assumed to be constant. The noise is reduced using a median filter and is then subtracted from the original image. The noise remains constant, while the signal is strongly depending on the visual context of the image, namely the distance to the target and the illumination conditions. Furthermore, the SNR was computed using an ISO 12233 pattern. A SNR of 56.7 dB was computed for the Close-Range Camera and 58.4 dB for the Mid-Range Camera. Naturally, this marks the maximal value and the SNR of the images recorded during the EPOS tests was well below these values.

Fig. 10 shows the signal to noise ratio of over the distance for the VIBANASS Close-Range Camera. The SNR increases with decreasing distance, as the camera is designed for distances shorter than 5 m and the size of the target seen by the camera and thus the signal level increases.

Bad illumination conditions included situations with no Target Illumination System or with bad sun angles and therefore poor illumination of the target and a poor signal. At distances below 2.1 m the chaser starts to shadow parts of the target. This leads to a sudden worsening of the illumination conditions and a strong divergence between good and bad illumination conditions.

Fig. 11 shows the SNR for the Mid-Range Camera, which is designed for distances larger than 5 m. Here, only a weak relation between the SNR and the distance can be identified. In contrast to the Close-Range Camera, the dependence on the illumination conditions is weaker, as it is easier to optimize the images by adjusting the exposure time. Further, the illumination conditions are more constant due to the lower amount of stray light and shadows and on the target.

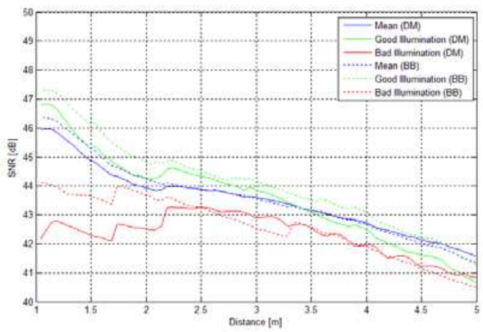

Figure 10. SNR over the distance for CAM-CR

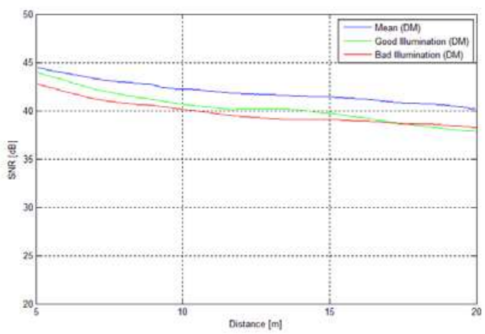

Figure 11. SNR over the distance for CAM-MR

4.3 Evaluation of Image Processing

This section describes the results of the image processing algorithm applied on the recorded test images. Before the actual image processing was performed, the cameras were calibrated using a chessboard pattern. Based on the results of the calibration, the extrinsic and intrinsic camera parameters have been computed and applied during the image processing.

Some general results of the tracking algorithm are shown in Fig. 12. The top row shows the results of the tracking in mid-range at 20 m and at 5 m, where the tracking target is the rectangular target shape. In close- range, the circular nozzle ring is the target of the tracking algorithm. As stereo images are used, the left and right camera images are shown at a distance of 5 m. The additional delay induced by the image processing software was measured with 130 ms on average.

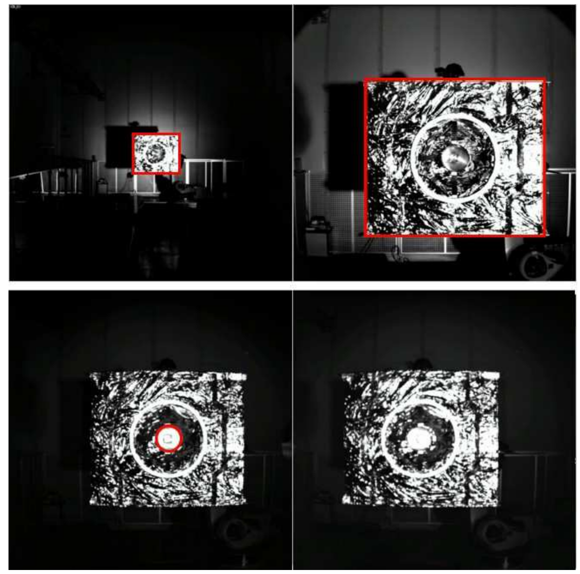

Figure 12. General results of image processing

For the actual evaluation of the image processing software, the stereo and the mono setup were tested and the error between the estimations and the values recorded by EPOS was computed. The relative error is defined as the relation between the position error in all three spatial dimensions with respect to the distance in percent.

Fig. 13 shows the resulting error of an approach under good illumination conditions. The relative error remains constant over the whole distance. In this case, the error ranges between 1% and 2%.

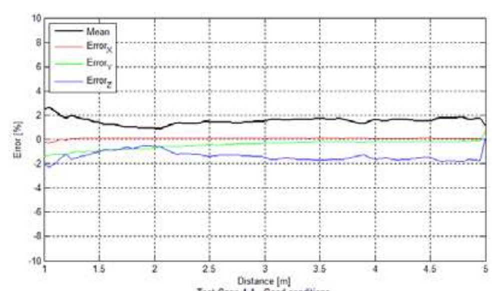

Figure 13. Result of tracking for good illumination conditions

An approach under bad illumination conditions is shown in Fig. 14. The absolute error is quite large and is further oscillating. Again, it decreases with decreasing distance. While the distance error in z-direction was dominant in test case T1.1 (see Fig. 12), the error in y- direction is dominant in this test case.

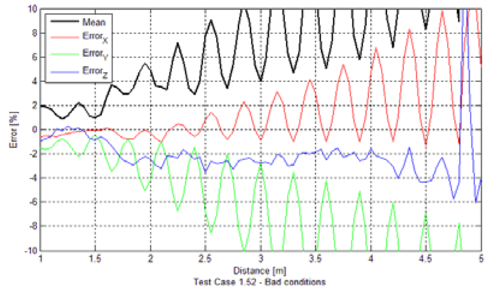

Figure 14. Result of tracking for bad illumination conditions

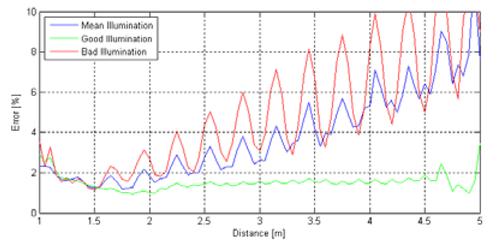

Figure 15. Impact of illumination conditions

Fig. 15 shows the relative error for the stereo algorithm. In all cases, the absolute error decreases with decreasing distance. The relative error has a more interesting behavior. It remains constant under good illumination conditions and decreases for average and bad illumination conditions.

The decrease can easily be explained, as the irradiance of the Target Illumination System increases with decreasing distance and the TIS becomes more dominant compared to the sunlight. However, at distances below 2.1 m the error begins to increase for all three cases. This behavior was also observed at the image quality factors and is explained by increasing stray light and shadows on the target induced by the chaser.

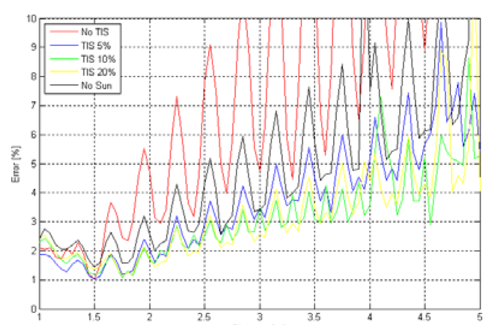

Figure 16. Impact of the Target Illumination System

The impact of the brightness of the TIS is shown in Fig. 16. "No TIS" shows the worst performance, while the active modes are comparable. When the target is illuminated only by the TIS, the resulting performance is slightly worse than when both sun and TIS are active. These tests show that the TIS is mandatory for the image processing algorithm, as it significantly increases the brightness of the image, revealing more details of the target and illuminating shadowed parts.

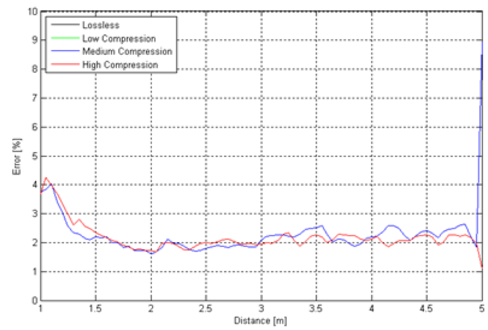

Figure 17. Impact of image compression

As described before, image compression has a large impact on the image quality. High compression rates, as they are required for GEO applications, lead to large artifacts and poor quality. Thus, the error of image processing under different image compression settings is of great interest.

To investigate this, several trajectories under good illumination conditions have been repeated with different compression settings. Fig. 17 shows the result of the stereo image processing algorithm in Close-Range. The resulting error is independent from the compression, proving that a vision-based approach is possible even with a small communication bandwidth.

4.4 Closed-Loop Tests

In the tests described so far, trajectories have been run and the images have been recorded for later evaluation. Since the computed relative error was within the specified limits, it was considered possible to use the result of the position estimation as input for additional closed-loop tests.

Similar to the open-loop tests, EPOS was used to simulate the environment with realistic illumination conditions. A software based simulator was integrated, containing dynamic models of the two satellites and a guidance, navigation and control (GNC) system using the results from VIBANASS as input for its navigation filter. The dynamic model simulates orbit controller, actuators and sensors, orbit dynamics and kinematics, and delivers the position and pose of the two satellites. This was then used as input for the robot control of the EPOS facility, closing the control loop.

A modified version of the N1 trajectory was used for the closed-loop tests with decreased speed and a longer hold point at 5 m. Due to safety reasons, the end point was moved to a distance of 2 m between chaser and target. The switch between mid- and close-range was done manually.

A selection of seven different illumination conditions from the good and average conditions have been tested. In an additional test, the image processing software was replaced with an operator performing its tasks.

5 SUMMARY

The VBIANASS Demonstrator Model tests at the European Proximity Operations Simulator (EPOS) were completed with great success as the Camera System Demonstrator Model, the Target Illumination System Demonstrator Model and the Ground Operation System were tested successfully.

An analysis of the impact of the illumination conditions on the accuracy of the tracking algorithm has shown that the Target Illumination System improves the natural illumination conditions such that the distance determination requirements can be fulfilled.

Under good illumination conditions, the tracking algorithm is able to estimate the position of the target with an accuracy of ~1%. This tracking algorithm is still able function with an adequate error using highly compressed images.

Finally, the functionality of VIBANASS and the image processing software could be proven during additional closed-loop tests. During these tests, the result of the image processing algorithm was used as control input for a rendezvous simulator.

It could be shown during the EPOS test campaign that VIBANASS is a capable optical sensor for Rendezvous and Docking applications in mid- and close-range. The Target Illumination System significantly decreases the dependence on natural illumination, allowing to use VIBANASS under a wide variety of environmental conditions.

Since VIBANASS can also be used for target inspection, it is excellently suited for ADR missions or precursor missions such as DEOS [7].

6 ACKNOWLEDGMENTS

VIBANASS is a Kayser-Threde development programme under co-funding by the German DLR Space Agency (Förderkennzeichen 50RA1001) and is being carried out in cooperation with DLR-RM (DLR Institute for Mechatronics and Robotics) and DLR-RB (DLR Institute for Space Operations and Astronaut Training). vH&S (von Hörner & Sulger) is subcontractor to Kayser-Threde.

7 REFERENCES

1. Krag, H. & Virgili, B. (2012). Removal Target Selection and its Environmental Effect. Presentation at Cleanspace Workshop on Active Space Debris Removal, ESCO, Darmstadt, 17-18 September 2012.
2. Rank, P. & Kaiser, C. (2010). *VIsion BAsed Navigation Sensor System VIBANASS*, AGASSE
3. Kaiser, C. & Rank, P. & Landzettel, K. & Boge, T. & Turk, M. (2011). *Vision Based Navigation for Future on-Orbit Servicing Missions*, 62nd International Astronautical Congress
4. Mühlbauer, Q. & Richter, L. & Kaiser, C. & Hofmann, P. (2012). *Robotics Space Systems and Subsystems for Advanced Future Programmes* International Symposium on Artificial Intelligence, Robotics and Automation in Space (i-SAIRAS)
5. Wimmer T., & Boge, T. & Mühlbauer, Q. (2011). EPOS: A Hardware-in-the-Loop Robotic Simulation Assembly for Testing Automated Rendezvous and Docking GNC Sensor Payloads. International ESA Conference on Guidance, Navigation & Control Systems
6. Oumer, N. & Panin, G. (2012) *3D point tracking and pose estimation of a space object using stereo images*, IAPR International Conference on Pattern Recognition (ICPR)
7. Rank, P. & Mühlbauer, Q. & Naumann, W. & Landzettel, K. (2011). The DEOS Automation and Robotics Payload, 11th Symposium on Advanced Space Technologies in Robotics and Automation